

The dispersion relation of rho meson in hot/dense nuclear matter

Ji-sheng Chen^a Jia-rong Li^b Peng-fei Zhuang^a

^a*Physics Department, Tsinghua University, Beijing 100084, P.R. China*

^b*Institute of Particle Physics, Hua-Zhong Normal University, Wuhan 430079, P.R.China.*

Abstract

The dispersion relation of ρ meson in hot/dense medium is analyzed based on the quantum hadrodynamics model with random phase approximation. The real mass and Debye mass behaviors of ρ meson and σ are discussed and compared. The effective masses of ρ and N decrease with the increase of density. The behaviors of Debye masses m_ρ^{s*} and m_σ^{s*} vs density are quite different, which reflect the characteristics of scalar σ and vector ρ mesons, respectively.

PACS: 14.40. Cs, 11.55. Fv, 11.10. Wx

Keywords:Vector meson, Dispersion relation, Finite temperature field theory

Heavy ion collision physics has excited wide investigation about the properties of strongly interacting matter in hot/dense nuclear environment [1]. Among the proposed signals for detecting the hot/dense matter associated with the quark-hadron phase transition formed in the heavy ion collisions the dileptons and photons are considered to be the clearest ones because they can penetrate the medium almost undisturbed and can reflect the property of the fireball formed in the initial stage of collision [2–4]. Even on the hadronic matter level, the masses of hadrons will be reduced as the result of the partial chiral symmetry restoration and the dileptons from the decay of light vector mesons, such as ρ , ω , ϕ are also considered to be the good signals of the partial chiral symmetry restoration. The study about the property of light vector mesons in extreme conditions is an important topic in

heavy ion physics, which also contributes to the studying of compact stellar objects such as the neutron stars [5].

The property of ρ in hot/dense environment was widely discussed in the literature due to its relative larger decay width compared with ω or ϕ [6,7]. Among the results about the property of ρ , esp. about its effective mass in medium, the famous is the decreasing mass conjecture made by Brown and Rho [8], which can be used to explain the low invariant mass dilepton enhancement in the central $A - A$ collisions observed by CERES-NA45 [9,10]. However, the conclusion of study about the ρ meson property in hot/dense environment is not unique and even some controversy results have also been obtained [11–15]. The property of ρ in extreme conditions is not clear and deserves further study.

The collective effects of the environment on ρ is reflected by its full propagator, which determines its dispersion relation as well as the response to external source [16,17]. Due to the broken Lorentz symmetry, the dispersion relations for the longitudinal and transverse modes are different, which are quite different from the vacuum occasion [16]. Here we attempt a study about the dispersion relation of ρ based on the quantum hadrodynamics model (QHD) [18,17]. With a hadronic effective theory, the vector meson effective masses esp. the Debye (or screening) masses at $T = 0$ occasion have been discussed by Shiomi et al. in Refs. [11]. Here we extend their works to finite temperature. The real mass and the Debye masses as well as the dispersion relation of ρ and σ are analyzed by calculating the self-energy in medium with the Random Phase Approximation (RPA). The dispersion curve of ρ including the Debye masses as well as the real mass is given. We find that the behavior of the σ Debye mass vs baryon density is quite controversy to that of ρ , which reflects the characteristic of vector and scalar mesons in QHD.

We start from the original QHD-I (Walecka Model) to obtain the required effective nucleon mass and effective chemical potential for the discussing of ρ property. The QHD-I Lagrangian including the freedoms of nucleon ψ , ω meson V as well as the scalar meson ϕ is [18–20]

$$\mathcal{L} = \bar{\psi} [\gamma(i\partial^\mu - g_\omega V^\mu) - (M_N - g_\sigma \phi)] \psi + \frac{1}{2} (\partial_\mu \partial^\mu \phi - m_\sigma^2 \phi^2) - \frac{1}{4} F_{\mu\nu} F_{\mu\nu} + \frac{1}{2} m_\omega^2 V_\mu V^\mu + \delta L, \quad (1)$$

where the δL represents the renormalization counterterm within the Relativistic Hartree Approximation (RHA) [18]. The basic characteristic of this model is that the nucleons interact with each other through the exchange of scalar σ and vector ω meson. With the mean field approximation, the effective nucleon mass M_N^* and effective chemical potential μ^* are determined by the pole position of the full nucleon propagator. By taking into account the vacuum fluctuation through the σ and ω meson tadpole diagrams, the self-consistent equations for the effective nucleon mass M_N^* and the effective chemical potential μ^* are [18]

$$M_N^* - M_N = -\frac{g_\sigma^2}{m_\sigma^2} \rho_s + \frac{g_\sigma^2}{m_\sigma^2} \frac{1}{\pi^2} \left[M_N^{*3} \ln\left(\frac{M_N^*}{M_N}\right) - M_N^2 (M_N^* - M_N) - \frac{5}{2} M_N (M_N^* - M_N)^2 - \frac{11}{6} (M_N^* - M_N)^3 \right], \quad (2)$$

$$\mu^* - \mu = -g_\omega^2 \rho_B / m_\omega^2, \quad (3)$$

where the baryon density ρ_B and scalar density ρ_s are determined by

$$\rho_B = \frac{4}{(2\pi)^3} \int d^3\mathbf{k} [n_B(\mu^*, T) - \bar{n}_B(\mu^*, T)], \quad (4)$$

$$\rho_s = \frac{4}{(2\pi)^3} \int d^3\mathbf{k} [n_B(\mu^*, T) + \bar{n}_B(\mu^*, T)],$$

with the Fermi-Dirac distribution functions

$$n_B(\mu^*, T) = \frac{1}{e^{\beta(\omega - \mu^*)} + 1}, \quad \bar{n}_B(\mu^*, T) = \frac{1}{e^{\beta(\omega + \mu^*)} + 1}. \quad (5)$$

The above coupled equations can be solved numerically with the parameters in Tab. I [18,19]. The M_N^* decreases with the increase of density ρ_B with fixed temperature. For example, M_N^* decreases to about 76% of the vacuum mass for $\rho = \rho_0$ with $T = 100$ MeV. For fixed density, the behavior of the M_N^* vs temperature is complicated more. Taken $\rho_N/\rho_0 = 1.5$ for example, M_N^* increases before $T = 118$ MeV and then decreases with the increase of T . The influence of temperature on the intermediate quantity-effective chemical potential μ^* is evident, which can affects the property of meson in medium indirectly through the nucleon loop.

The full propagator of rho meson determines the property in medium, which is analyzed by using the random phase approximation. The Dyson-equation of the ρ meson propagator is consisted of repeated insertions of the polarizations. The solution of Dyson-equation is that the full propagator ($D^{\mu\nu}$) can be determined by the polarization tensor $\Pi^{\mu\nu}(k)$ with

$$\Pi^{\mu\nu}(k) = (D^{-1})^{\mu\nu} - (D_{(0)}^{-1})^{\mu\nu}. \quad (6)$$

The $D_{(0)}^{\mu\nu}$ is the bare propagator. Different from the vacuum occasion in vacuum, there are two independent elements $\Pi_{L(T)}$ for the tensor $\Pi^{\mu\nu}(k)$ determined by

$$\Pi_L(k) = \frac{k^2}{\mathbf{k}^2} \Pi^{00}(k), \quad \Pi_T(k) = \frac{1}{2} P_T^{ij} \Pi_{ij}(k), \quad (7)$$

where the $P_L^{\mu\nu}$ and $P_T^{\mu\nu}$ are the standard projection tensors [16]. The pole position of the full propagator $D^{\mu\nu}$ completely determines the dispersion relation of rho meson excitations in medium,

$$k^2 - m_\rho^2 - \Pi_{L(T)}(k) = 0, \quad (8)$$

while its imaginary part gives the spectral function [7,21].

With the obtained M_N^* and μ^* , the polarization tensor $\Pi^{\mu\nu}(k)$ is calculated according to the Feynman rules given by the following effective Lagrangian [11,22]

$$\mathcal{L}_{\rho NN} = g_{\rho NN} (\bar{\Psi} \gamma_\mu \tau^a \Psi V_a^\mu - \frac{\kappa_\rho}{2M_N} \bar{\Psi} \sigma_{\mu\nu} \tau^a \Psi \partial^\nu V_a^\mu), \quad (9)$$

where V_a^μ is the ρ meson field and Ψ the nucleon field. In the imaginary time formalism, it is given by [16]

$$\Pi^{\mu\nu}(k) = 2g_{\rho NN}^2 T \sum_{p_0} \int \frac{d^3 \mathbf{p}}{(2\pi)^3} \text{Tr} \left[\Gamma^\mu(k) \frac{1}{\not{p} - M_N^*} \Gamma^\nu(-k) \frac{1}{(\not{p} - \not{k}) - M_N^*} \right], \quad (10)$$

where $\Gamma^\mu = \gamma^\mu + \frac{ik_\rho}{2M_N} \sigma^{\mu\nu} k_\nu$ with the 0-component of the on-loop nucleon momentum related to the temperature T and effective chemical potential μ^* via $\bar{p}_0 = (2n+1)\pi T i + \mu^*$. With the residue theorem, one can separate the polarization tensor into two parts

$$\Pi^{\mu\nu}(k) = \Pi_{\text{P}}^{\mu\nu}(k) + \Pi_{\text{D}}^{\mu\nu}(k). \quad (11)$$

The first part $\Pi_F^{\mu\nu}(k)$ corresponds to the particle-antiparticle contribution of the Dirac sea in the $T = 0$ occasion, while the second part $\Pi_D^{\mu\nu}(k)$ to the particle-hole contribution [11,17]. Due to the tensor-coupling part of the vertex Γ_μ , $\Pi_F^{\mu\nu}$ containing divergent integrals can not be renormalized by conventional method. After separating the divergent part of $\Pi_F^{\mu\nu}$ with the dimension regularization method, we apply the following phenomenological renormalization method to reflect the medium contribution by subtracting the finite vacuum contribution [11,23–25]

$$\partial^n \Pi_F(k) / \partial(k^2)^n |_{M_N^* \rightarrow M_N, k^2 = m_\rho^2} = 0, \quad (n = 0, 1, 2, \dots, \infty), \quad (12)$$

with

$$\Pi_F^{\mu\nu}(k) = \left(\frac{k^\mu k^\nu}{k^2} - g^{\mu\nu} \right) \Pi_F(k), \quad (13)$$

$$\Pi_F(k) = k^2 \frac{g_{\rho NN}^2}{\pi^2} \left(P_1 + \frac{\kappa_\rho}{2M_N} M_N^* P_2 + \left(\frac{\kappa_\rho}{2M_N} \right)^2 \frac{k^2 P_1 + M_N^{*2} P_2}{2} \right), \quad (14)$$

$$\begin{aligned} P_1 &= \int_0^1 dx x(1-x) \ln c, & P_2 &= \int_0^1 dx \ln c, \\ c &= \frac{M_N^{*2} - x(1-x)k^2}{M_N^{*2} - x(1-x)k^2}. \end{aligned}$$

The calculation of the second part $\Pi_D^{\mu\nu}(\mu^*, T)$ for the polarization tensor is much more involved and the expression is very lengthy. We list the final results in the appendix. To obtain the final physical result, one must do the analytical continuation $k_0 \rightarrow k_0 + i\varepsilon^+$ to the results obtained in the imaginary time formalism [7,16].

For vector meson excitations in the medium, the dispersion relations of longitudinal and transverse mode are different. However, the real masses determined by taking the limit $|\mathbf{k}| \rightarrow 0$ for L and T modes are the same

$$k_0^2 - m_\rho^2 - \lim_{|\mathbf{k}| \rightarrow 0} \Pi_{L(T)}(k) = 0, \quad (15)$$

with $\Pi^{L(T)}(k) = \Pi_F^{L(T)}(k) + \Pi_D^{L(T)}(k)$.

The difference between L and T modes can be seen clearly by the corresponding different Debye masses. The Debye mass is defined as the inverse Debye screening length. Just like

the real mass, the Debye masses reflect the collective effects of the medium on the ρ meson property, which are obtained by taking the limit $k_0 \rightarrow 0$ (Here, the wave numbers are purely imaginary numbers and related to the Debye masses M_D 's through $M_D = -iK$),

$$\mathbf{k}^2 + m_\rho^2 + \Pi^{L(T)}(k)|_{k_0=0} = 0. \quad (16)$$

They describe the damping characteristic $e^{-|\mathbf{k}|x}$ of the excitations [11,16]. As shown in the left panel of Fig.1 the difference between the L and T mode Debye masses for ρ is evident. For comparison of their varying tendency with density ρ_B , the effective nucleon mass curve is also drawn out.

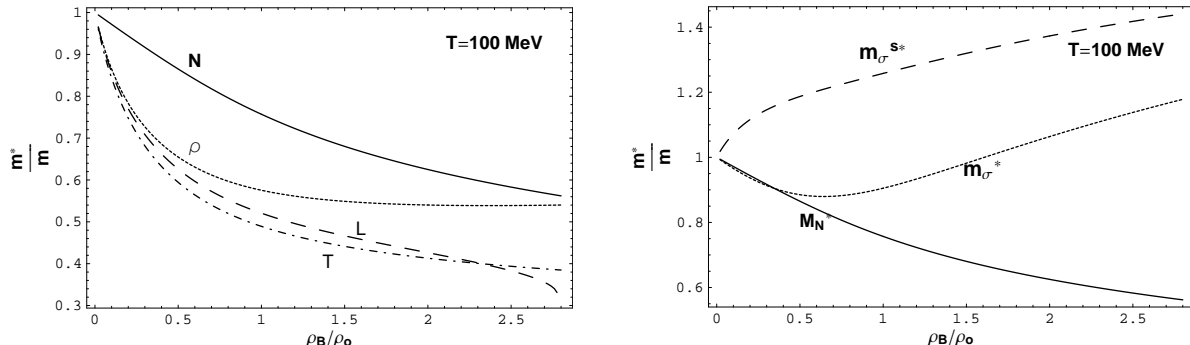


FIG. 1. The effective masses M_N^* , m_ρ^{s*} , m_ρ^* (left panel) and m_σ^* , m_σ^{s*} (right panel) vs density with $T = 100$ MeV, respectively. Left panel: the solid line corresponds to the effective nucleon mass M_N^* , the dotted line to the real mass m_ρ^* and dashed to $m_{\rho,L}^{s*}$ and dot-dashed to the $m_{\rho,T}^{s*}$ screening mass of ρ , respectively. Right panel: the solid line is still the nucleon curve, while dotted line corresponds to the real mass m_σ^* and dashed line to screening mass m_σ^{s*} of σ meson, respectively.

It is interesting to discuss the property of the scalar meson σ with QHD and compare the results with those for the vector mesons. At zero-temperature and hadronic model, the property of σ has been discussed in such as Refs. [26,27]. However, the screening mass of σ has not been discussed for both zero-temperature and finite-temperature before. Here we extend to finite temperature occasion and discuss the behavior of its screening mass vs the baryon density. At finite temperature, the self-energy of σ meson is determined by the Feynman rules obtained from the original Langrian (1)

$$\Pi_\sigma(k) = 2g_\sigma^2 \sum_{p_0} \int \frac{d^3\mathbf{p}}{(2\pi)^3} \text{Tr} \left[\frac{1}{\not{p} - M_N^*} \frac{1}{(\not{p} - \not{k}) - M_N^*} \right]. \quad (17)$$

Analogously to the calculation of the ρ meson polarization, one can obtain

$$\begin{aligned} \Pi_\sigma(k) = & \frac{3g_\sigma^2}{2\pi^2} \left[3(M_N^{*2} - M_N^2) - 4(M_N^* - M_N)M_N \right. \\ & - (M_N^{*2} - M_N^2) \int_0^1 \ln \frac{M_N^{*2} - x(1-x)k^2}{M_N^2} dx \\ & \left. - \int_0^1 (M_N^2 - x(1-x)k^2) \ln \frac{M_N^{*2} - x(1-x)k^2}{M_N^2 - x(1-x)k^2} dx \right] \\ & + \frac{g_\sigma^2}{\pi^2} \int \frac{p^2 dp}{\omega} (n_B(\mu^*, T) + \bar{n}_B(\mu^*, T)) \left[2 + \frac{k^2 - 4M_N^{*2}}{4p|\mathbf{k}|} (\ln a + \ln b) \right], \end{aligned} \quad (18)$$

where

$$\omega = \sqrt{p^2 + M_N^{*2}}, \quad (19)$$

$$a = \frac{k^2 - 2p|\mathbf{k}| - 2k_0\omega}{k^2 + 2p|\mathbf{k}| - 2k_0\omega}, \quad b = \frac{k^2 - 2p|\mathbf{k}| + 2k_0\omega}{k^2 + 2p|\mathbf{k}| + 2k_0\omega}. \quad (20)$$

The numerical results of the real and screening masses of σ meson in the medium are indicated in the right panel of Fig. 1.

The behavior differences of real masses m_ρ^* , M_N^* and m_σ^* vs T (or ρ_B) for fixed ρ_B (or T) are evident. For example, from the left panel of Fig.1 for the case $T = 100$ MeV, one can see that both the effective ρ and nucleon masses decrease with the density. This decreasing tendency for other temperatures is similar and consistent with the Brown-Rho scaling result. However, one can see that the real mass m_σ^* decreases with the increase of ρ_B at first and then increases, which is not consistent with the conjecture of Brown-Rho. Especially, one can see that the Debye mass of sigma meson increases with the density, which characterizes the difference of scalar and vector meson in QHD.

From Eq.(8), one can draw out the corresponding dispersion curves. The difference between the almost coincided L and T dispersion curves can be reflected by the corresponding Debye masses as shown in Fig.2. It is also interesting to find that the invariant mass $\sqrt{k_0^2 - \mathbf{k}^2}$ of ρ meson in medium is almost a constant, which is indicated in the Fig. 2 by the dashed-lines. One can give the dispersion curve of σ similarly.

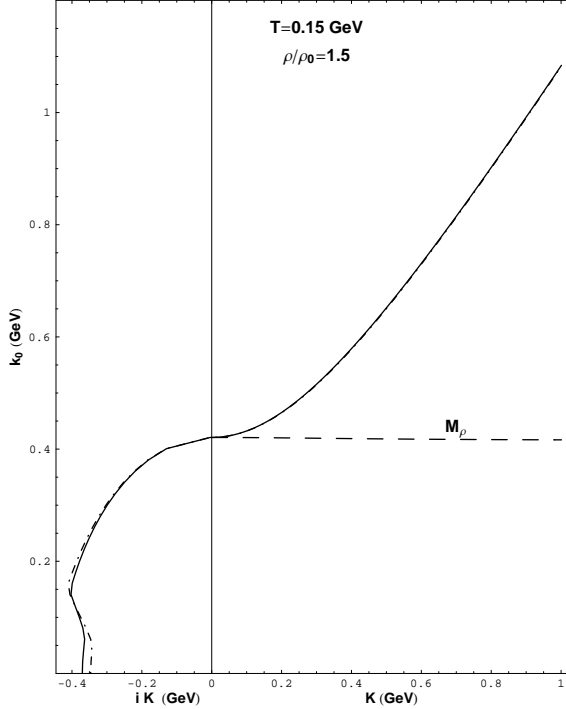


FIG. 2. The dispersion curve for ρ meson, $T = 150$ MeV and $\rho_B/\rho_0 = 1.5$. The solid line corresponds to L mode, dot-dashed to T and long-dashed to invariant mass $M_\rho = \sqrt{k_0^2 - \mathbf{k}^2}$.

In summary, we analyzed the dispersion relation of ρ as well as σ in hot/dense environment with RPA. The effective masses (real and screening masses) of ρ meson are found to decrease with the increase of the density. The difference of the L and T Debye masses is obvious, which is indicated by the drawn dispersion curves of L and T modes including the Debye masses. Compared with the increased Debye mass of σ vs the density, the decreased Debye masses of ρ indicate that the vector mesons become more important in high density occasion and can be considered as the signal of the density effect from the point of meson exchange view [22,28,29], which affects the property of nuclear matter [30]. The influence of the modified ρ property in hot/dense environment on the dilepton spectrum deserves further study and work on this respect is in progress.

TABLE I. The parameters used in this work. The nucleon mass, the ω -meson and ρ -meson masses are fixed at their physical values ($M_N = 939$ MeV, $m_\omega = 783$ MeV, $m_\rho = 770$ MeV).

parameters	g_σ^2	g_ω^2	m_σ (MeV)	$g_{\rho NN}$	k_ρ
values	54.289	102.770	458	2.63	6.1

APPENDIX A

The results of $\Pi_D^{\mu\nu}$ corresponding to the Fermi-sea contribution of zero-temperature occasion are related obviously to the distribution functions $n_B(\mu^*, T)$ and $\bar{n}_B(\mu^*, T)$. In this appendix, the ingredients are given out.

The 00 elements:

$$\begin{aligned}
 \Pi_D^{00}(k) &= \Pi_{1D}^{00} + \Pi_{2D}^{00} + \Pi_{3D}^{00}, \\
 \Pi_{1D}^{00} &= -2\left(\frac{g_{\rho NN}}{2\pi}\right)^2 \int \frac{p^2 dp}{\omega} (n_B(\mu^*, T) + \bar{n}_B(\mu^*, T)) \\
 &\quad \left(4 + \frac{k^2 - 4\omega k_0 + 4\omega^2}{2p|\mathbf{k}|} \ln a + \frac{k^2 + 4\omega k_0 + 4\omega^2}{2p|\mathbf{k}|} \ln b\right), \\
 \Pi_{2D}^{00} &= 4|\mathbf{k}|\left(\frac{g_{\rho NN}}{2\pi}\right)^2 \frac{k_\rho}{2M_N} M_N^* \int \frac{p dp}{\omega} (n_B(\mu^*, T) + \bar{n}_B(\mu^*, T)) (\ln a + \ln b), \\
 \Pi_{3D}^{00} &= 2\left(\frac{g_{\rho NN}}{2\pi}\right)^2 \left(\frac{k_\rho}{2M_N}\right)^2 \int \frac{p^2 dp}{\omega} (n_B(\mu^*, T) + \bar{n}_B(\mu^*, T)) \\
 &\quad \left[4k_0^2 + \frac{\mathbf{k}^2(k^2 - 4p^2) + (k^2 - 2k_0\omega)^2}{2p|\mathbf{k}|} \ln a\right. \\
 &\quad \left. + \frac{\mathbf{k}^2(k^2 - 4p^2) + (k^2 + 2k_0\omega)^2}{2p|\mathbf{k}|} \ln b\right].
 \end{aligned} \tag{A1}$$

The $0i$ elements:

$$\Pi_D^{0i}(k) = \frac{k^0 k^i}{\mathbf{k}^2} \Pi_D^{00}(k). \tag{A2}$$

The ij elements:

$$\begin{aligned}
 \Pi_D^{ij}(k) &= (A_1 + A_2 + A_3)\delta^{ij} + (B_1 + B_2 + B_3)\frac{k^i k^j}{\mathbf{k}^2}, \\
 A_1 &= \left(\frac{g_{\rho NN}}{2\pi}\right)^2 \int \frac{p^2 dp}{\omega} (n_B(\mu^*, T) + \bar{n}_B(\mu^*, T)) \\
 &\quad \left[\frac{4(\mathbf{k}^2 + k_0^2)}{\mathbf{k}^2} - \frac{\mathbf{k}^4 - k_0^2(k_0 - 2\omega)^2 + 4\mathbf{k}^2(p^2 - k_0\omega)}{2p|\mathbf{k}|^3} \ln a\right]
 \end{aligned} \tag{A3}$$

$$-\frac{\mathbf{k}^4 - k_0^2(k_0 + 2\omega)^2 + 4\mathbf{k}^2(p^2 + k_0\omega)}{2p|\mathbf{k}|^3} \ln b \Big],$$

$$A_2 = \frac{k^2}{\mathbf{k}^2} \Pi_{2D}^{00},$$

$$A_3 = -k^2 \left(\frac{g_{\rho NN}}{2\pi} \right)^2 \left(\frac{k_\rho}{2M_N} \right)^2 \int \frac{p^2 dp}{\omega} (n_B(\mu^*, T) + \bar{n}_B(\mu^*, T)) \left[4 \frac{k^2}{\mathbf{k}^2} + \frac{k^4 + 4k^2\omega(\omega - k_0) + 4\mathbf{k}^2(p^2 - \omega^2)}{2p|\mathbf{k}|^3} \ln a \right. \\ \left. + \frac{k^4 + 4k^2\omega(\omega + k_0) + 4\mathbf{k}^2(p^2 - \omega^2)}{2p|\mathbf{k}|^3} \ln b \right],$$

$$B_1 = \left(\frac{g_{\rho NN}^2}{2\pi} \right)^2 \int \frac{p^2 dp}{\omega} (n_B(\mu^*, T) + \bar{n}_B(\mu^*, T)) \left[-4 \frac{(\mathbf{k}^2 + 3k_0^2)}{\mathbf{k}^2} + \frac{\mathbf{k}^4 - 3k_0^2(k_0 - 2\omega)^2 + 2\mathbf{k}^2(k_0^2 + 2p^2 - 2k_0\omega)}{2p|\mathbf{k}|^3} \ln a \right. \\ \left. + \frac{\mathbf{k}^4 - 3k_0^2(k_0 + 2\omega)^2 + 2\mathbf{k}^2(k_0^2 + 2p^2 + 2k_0\omega)}{2p|\mathbf{k}|^3} \ln b \right],$$

$$B_2 = \Pi_{2D}^{00},$$

$$B_3 = \left(\frac{g_{\rho NN}}{2\pi} \right)^2 \left(\frac{k_\rho}{2M_N} \right)^2 \int \frac{p^2 dp}{\omega} (n_B(\mu^*, T) + \bar{n}_B(\mu^*, T)) \left[4 \frac{(k_0^4 + k^4)}{\mathbf{k}^2} \right. \\ \left. + \frac{k^2(2k_0^4 + k^4) + 4k_0k^2(2k_0^2 + k^2)\omega - 4(2\mathbf{k}^2 + k^2)\mathbf{k}^2p^2 + 4(2k_0^4 - k_0^2k^2 + 2k^4)\omega^2}{2p|\mathbf{k}|^3} \ln a \right. \\ \left. + \frac{k^2(2k_0^4 + k^4) - 4k_0k^2(2k_0^2 + k^2)\omega - 4(2\mathbf{k}^2 + k^2)\mathbf{k}^2p^2 + 4(2k_0^4 - k_0^2k^2 + 2k^4)\omega^2}{2p|\mathbf{k}|^3} \ln b \right],$$

where the expressions of ω , a and b are similar to those in Eq.(18).

For example, from Eq.(A3) one can obtain

$$\Pi_D^T(k) = A_1 + A_2 + A_3. \quad (\text{A4})$$

REFERENCES

- [1] R. Rapp and J. Wambach, *Adv. Nucl. Phys.* **25** (2000) 1[hep-ph/9909229].
- [2] K. Kajantie, J. Kapusta, Larry D. McLerran and A. Mekjian, *Phys.Rev.***D34** (1986) 2746.
- [3] I. Tserruya, *Nucl.Phys.***A590** (1995) 127c.
- [4] E. V. Shuryak, *Phys. Lett.* **B78** (1978) 150.
- [5] N.K. Glendenning, *Compact Stars: Nuclear Physics, Particle Physics, and General Relativity*, Springer (1997, New York, USA).
- [6] O. Teodorescu, A. K. Dutt-Mazumder and C. Gale, *Phys. Rev.* **C66** (2002) 015209[nucl-th/0112035].
- [7] C. Gale and J.I. Kapusta, *Nucl. Phys.* **B357** (1991) 65.
- [8] G. E. Brown and M. Rho, *Phys. Rev. Lett.* **D66** (1991) 2720.
- [9] G. Agakichiev *et al.* , CERES collaboration, *Phys. Rev. Lett.* **D75** (1995) 1272.
- [10] P. Wurm, for the CERES collaboration, *Nucl. Phys.* **A590** (1995) 103c.
- [11] H. Shiomi and T. Hatsuda, *Phys. Lett.* **B334** (1994) 281[hep-ph/9404337].
- [12] K. Saito, T. Maruyama and K. Soutome, *Phys. Rev.* **C40** (1989) 407; K. Saito and A. W. Thomas, *Phys. Rev.* **C51** (1995) 2757[nucl-th/9410031].
- [13] S. Leupold, W. Peters and U. Mosel, *Nucl. Phys.* **A628** (1997) 311[nucl-th/9708016].
- [14] F. Klingl, N. Kaiser and W. Weise, *Nucl. Phys.* **A624** (1997) 527[hep-ph/9704398].
- [15] T. Hatsuda and S.H. Lee, *Phys. Rev.* **C51** (1992) R34.
- [16] J.I. Kapusta, *Finite Temperature Field Theory*, Cambridge University Press, 1989.
- [17] S.A. Chin, *Ann. Phys.* **108** (1977) 301.

- [18] B.D. Serot and J.D. Walecka, *Adv. Nucl. Phys.* **16** (1986) 1.
- [19] H.-C. Jean, J. Piekarewicz, A. G. Williams, *Phys. Rev.* **C49** (1994) 1981[*nucl-th*/9311005].
- [20] Ji-sheng Chen, Jia-rong Li and Peng-fei Zhuang, *nucl-th*/0202026.
- [21] H. A. Weldon, *Phys. Rev.* **D42** (1992) 2384.
- [22] R. Machleidt, K. Holinde and Ch. Elster, *Phys. Rep.* **149** (1987) 1; R. Machleidt, *Adv. Nucl. Phys.* **19** (1989) 189.
- [23] H. Kurasawa and T. Suzuki, *Nucl. Phys.* **A490** (1988) 571.
- [24] A. K. Dutt-Mazumder, B. Dutta-Roy and A. Kundu, *Phys. Lett.* **B399** (1997) 196[*hep-ph*/9605247]; S. Sarkar, J. Alam, P. Roy, A. K. Dutt-Mazumder, B. Dutta-Roy, B. Sinha, *Nucl. Phys.* **A634** (1998) 206[*nucl-th*/9712007].
- [25] T. Hatsuda, H. Shiomi, H. Kuwabara, *Prog.Theor.Phys.* **95** (1996) 1009[*nucl-th*/9603043].
- [26] Y. Iwasaki, H. Kouno, A. Hasegawa and M. Nakano, *Int.J.Mod.Phys.* **E9** (2000) 459[*nucl-th*/0008018].
- [27] J.C. Caillon and J. Labarsouque, *Phys. Lett.* **B311** (1993) 19[*nucl-th*/9306012].
- [28] S. Gao and Y.J. Zhang and R.K. Su, *Phys. Rev.* **C53** (1996) 1098; Y.J. Zhang, S. Gao and R.K. Su, *Phys. Rev.* **C56** (1997) 3336.
- [29] R. Rapp, R. Machleidt, J.W. Durso and G.E. Brown, *Phys. Rev. Lett.* **D82** (1999) 1827[*nucl-th*/9706006].
- [30] M. Matsuzaki, T. Tanigawa, *Phys. Lett.* **B445** (1999) 254[*nucl-th*/9803044].